PAPER

Nanoplatform-based analysis for the detection of HER3 and HER4 for gastric cancer diagnosis

To cite this article: Damaris-Cristina Gheorghe *et al* 2023 *Nanotechnology* **34** 345101

IOP Publishing Nanotechnology
Nanotechnology 34 (2023) 345101 (10pp) https://doi.org/10.1088/1361-6528/acd9d3

Nanoplatform-based analysis for the detection of HER3 and HER4 for gastric cancer diagnosis

Damaris-Cristina Gheorghe[1,2], Raluca-Ioana Stefan-Van Staden[1,2,*], Ruxandra-Maria Ilie-Mihai[1,*] and Paula Sfirloaga[3]

[1] Laboratory of Electrochemistry and PATLAB, National Institute of Research for Electrochemistry and Condensed Matter, 202 Splaiul Independentei Street, 060021 Bucharest-6, Romania
[2] Faculty of Chemical Engineering and Biotechnologies, Politehnica University of Bucharest, 1-7 Gheorghe Polizu Street, 011061 Bucharest, Romania
[3] National Institute of Research for Electrochemistry and Condensed Matter, Dr Aurel Paunescu Podeanu 144, 300569 Timisoara, Romania

E-mail: ralucavanstaden@gmail.com and i.ruxandra04@yahoo.com

Received 9 February 2023, revised 18 May 2023
Accepted for publication 30 May 2023
Published 12 June 2023

Abstract

Nanographene and α-cyclodextrin based sensors modified with gold nanoparticles and spheroidal copper were used to develop two stochastic sensors, which were then characterized and validated for the purpose of molecularly identifying and quantifying HER3 and HER4 in biological samples. In order to accomplish this goal, each of the stochastic sensors was incorporated in a nanoplatform. The two nanoplatforms were connected to a smartphone and recorded very low limits of determination (1×10^{-15} g ml^{-1}) and wide linear concentration ranges (1×10^{-15}–1×10^{-8} g ml^{-1}) when a potential of 170 mV versus Ag/AgCl was applied. This allowed for the molecular identification and quantification of HER3 and HER4 in patients with gastric cancer, as well as in healthy individuals.

Keywords: stochastic sensor, nanoplatforms, gastric cancer, smartphone detection, HER

(Some figures may appear in colour only in the online journal)

1. Introduction

Human epidermal growth factor receptors, also known as ErbB, are engaged in crucial signaling pathways, including those that govern cell development, proliferation, and death [1, 2]. The HER family consists of four members: HER1 (EGFR or ErbB1), HER2 (ErbB2), HER3 (ErbB3), and HER4 (ErbB4) [3]. Overexpression of HER has been associated with the development of malignant potential and a bad prognosis in a number of different types of cancer [4, 5]. However, recent studies have proven that heterodimerization of HER3 with HER1/HER2/HER4 triggers a signaling network that promotes tumor development and metastasis [6, 7].

Similar to EGFR and HER2, HER3 and HER4 expression was identified in 20.7% and 13.3% of gastric tumors [8]. Multiple studies have shown a negative association between high HER3 expression and survival [9]. However, HER4 in gastric cancer has only been studied sparingly so far, and its relevance as a prognostic marker remains unclear [10]. He *et al* found that overexpression of HER4 was associated with tumor-nodes-metastasis but not with survival [8].

Until now, there are some research studies [11–13] that involve electrochemical studies in analyzing the HER family in biological samples. The development of sensors for the detection and measurement of bioanalytes is a prospective application for functional nanomaterials, which have demonstrated that they are promising candidates in this field. The remarkable properties of nanomaterials based on cyclodextrins (CD) and derivatives of cyclodextrins ensure enhanced performance of the sensors in terms of sensitivity, selectivity, detection limit, response time, and multiplexing capability.

* Authors to whom any correspondence should be addressed.

Electrochemical sensors are versatile, inexpensive, and easy to transport, with high sensitivity and selectivity for a wide range of analytical uses. One of the most important and difficult phases is the production of the sensor electrode, which serves as the transducer element.

Since a disease's course might be altered by a prompt diagnosis, there has been a surge in the creation of portable biosensors in the recent decade that can be used for rapid and cheap clinical examination as diagnostics instruments capable of disease screening [14]. The lack of adequately equipped clinics is the largest barrier to the immediate use of biosensors, which would greatly simplify and speed up the diagnosis process. For this reason, researchers have recently concentrated on creating inexpensive sensor nanoplatforms that can biodetect a variety of analytes or biotargets quickly and on-the-go [15]. Based on the findings, these sensing platforms are excellent candidates for future medical technology development and represent a fantastic chance to broaden clinical analysis and screening.

The development of electrochemical sensors has made considerable use of graphene due to its many excellent features [16]. Graphene has also been used in a variety of other applications. These desirable qualities include a large surface area, strong conductivity, extremely good stability, and good thermal and mechanical capabilities, while at the same time it provides a metal-free support for the CDs and it is simple to manufacture. In addition, it has a high surface area. Supramolecular systems (calixarenes, cyclodextrins, etc) may be included into the sensor design to increase selectivity and sensitivity for the target analyte, and several of these materials have the potential to provide high sensitivity in electrochemical detection [17].

Many alternative cyclodextrin combinations have been tried, all with the goal of immobilizing the molecule on the surface of sensors. By taking this route, a CD array may be formed with the ability to bind and trap the target analyte, allowing a more precise and sensitive detection [18].

In addition to this, they are capable of incorporating a wide range of different guest molecules, a process known as inclusion complexation, which makes them interesting for use in the delivery of drugs, as adsorbent materials, and in the sensor development process, particularly in the adjustment of sensors to give rise to high selective electrochemical sensors [19].

The purpose of this paper was to investigate a set of two biomarkers, HER3 and HER4, that are not known as being specific to gastric cancer, because there is only a limited amount of information available regarding the connection between HER3 and HER4 and clinical pathological symptoms, as well as the role that HER3 and HER4 play in the development of gastric cancer (scheme 1). Nanoplatforms incorporating the stochastic sensors were utilized to achieve this objective. Gold nanoparticles (Au NPs) were chosen for the construction of the stochastic sensors because of their high stability, and high conductivity [20]. Limits of determination were determined accordingly with the requirements of IUPAC [21].

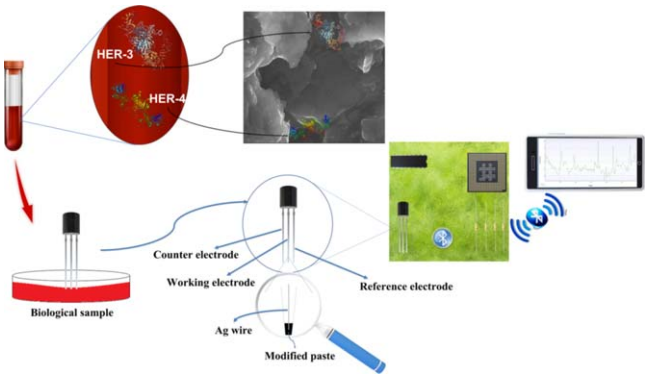

Scheme 1. Nanoplatform construction and set-up.

The innovative aspects of this article, compared with related work [22] are: the combination of nanoplatforms and smartphone detection; utilization of nanographene as matrix for the design of the stochastic sensors; utilization of nanoparticles of Au and of spheroidal Cu for modification of nanographene.

2. Materials and methods

2.1. Chemicals

In all phases of this experiment, analytical-grade compounds were utilized. HER3, HER4, α-cyclodextrine (α-CD), AuNPs, spheroidal copper (spheroidal Cu), the graphene nanopowder (nGr), and, as well as monosodium phosphate and disodium phosphate, were all purchased from Sigma Aldrich in Milwaukee, United States of America. The paraffin oil was obtained from Fluka (Buchs, Switzerland). Phosphate buffer (PBS) with a pH of 7.40 was prepared using monosodium phosphate and disodium phosphate. Using the procedure of serial dilution, the acquired PBS was utilized to produce HER3 and HER4 solutions. The concentrations of HER3 and HER4 in the solutions of interest ranged from 1.00 to 1.00×10^{-9} μg ml^{-1}. The prepared solutions were utilized for one month; while not in use, they were stored between 2 °C and 8 °C.

2.2. Instruments and methods

An EmStatpico apparatus from PalmSens (Houten, the Netherlands), which was linked to a laptop/smartphone running PSTrace software (Version 5.9), was utilized so that all measurements could be recorded. No Fraday cage and no stirring were used during the measurements. Additionally, a three-electrode electrochemical cell was utilized in the experiment, which represents the nanoplatform. The three-electrode system has working electrodes that are comprised of the stochastic sensors that were suggested. The reference electrode, which is also referred to as the Ag/AgCl electrode, and the counter electrode, which is a platinum wire, function, respectively, as the reference and counter electrodes.

Using scanning electron microscopy (SEM) (Inspect S), FEI Company Netherlands, a qualitative analysis of the

studied materials was conducted. To obtain the best image resolution, all samples were analyzed in high vacuum mode with an ETD detector, high voltage of 25 kV, a spot value of 2, and a magnification of 1600.

2.3. The stochastic sensors' and nanoplatforms' design

Nanographene powder and a solution of α-CD (10^{-3} mol l^{-1}) were used for the design of the two stochastic sensors. For the first sensor, 100 mg of nanographene was mixed with 100 μl α-CD solution (10^{-3} mol l^{-1}) and paraffin oil to make a homogenous paste. 10 μl of AuNPs were added to the paste. For the second sensor, to the modified nanographene paste, spheroidal Cu was added. Since the bare sensor (nanographene and AuNPs) didn't offer the stochastic signal of interest, α-CD was added to provide the channels that were needed to obtain the specific stochastic signals for the sensors.

The two pastes and the exterior circuit of the electrochemical cell were connected by a silver wire. Each paste was placed in nonconductive plastic tubes. The designed stochastic sensors were integrated into nanoplatforms (scheme 1). After every measurement, whether of solutions or biological samples, the measurement site of the platform was cleansed with deionized water and dried. These nanoplatforms sensors were stored in a dry place when not in use. Neither the solutions nor the biological samples were found to have contaminated the surface of the sensors which could have been used for more than 100 measurements per day.

2.4. Stochastic mode

The conductivity of the channel or pore underlies the stochastic sensor's working principles. The analyte modifies the ionic currents flowing through the pore, which was designed to contain binding sites. Each analyte produces a unique signature (t_{off}), which is influenced by its size, geometry, stereogeometry, capacity of unfolding, and velocity of passing through the channel/pore; thus, it is uncommon for two analytes to have the same signature. The frequency ($1/t_{on}$) of binding events reveals the concentration of the analyte, while the nature and duration of the binding events reveal its signature.

A chronoamperometric approach was used for the stochastic method when a constant voltage (170 mV versus Ag/AgCl) was applied. The choice of this potential was based on obtaining a reliable signal, with a measurable signature, taking into account that the value of the signature is decreasing with increasing the potential. The noise was eliminated from the diagrams before the reading of the signatures and t_{on} values; a ratio of 97:1 was determined for signal/noise. This method was applied to qualitatively and quantitatively assess HER3 and HER4 in whole blood and tumoral tissue samples from patients with proven gastric cancer. Using the proposed sensors, one can obtain specific diagrams in which the two parameters of interest, t_{off} and t_{on}, were identified (figures 1 and 2).

t_{off} is regarded as the analytes' signatures, and its values are utilized for qualitative analysis (it is the time needed for each biomarker to get inside the channel); during this time, the channel is blocked, and therefore, the current drops to zero; using the signature value, HER3 and HER4 were identified in the diagrams obtained for the assessment of biological samples (figures 1 and 2). t_{on} reflects the quantitative parameter and is known as the period of equilibrium necessary for the interaction of the analytes with the wall channels and the redox processes which occur within those channels (it is the time needed for completing the bonding and the redox processes inside the channel). During the redox

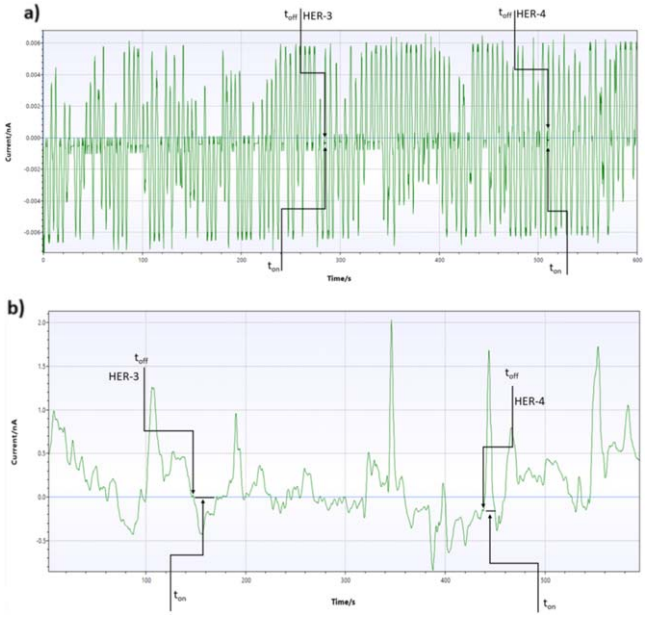

Figure 1. Examples of diagrams for the screening tests of whole blood using the stochastic sensors based on: (a) AuNPs/α-CD-nGr and (b) spheroidal Cu/α-CD-nGr.

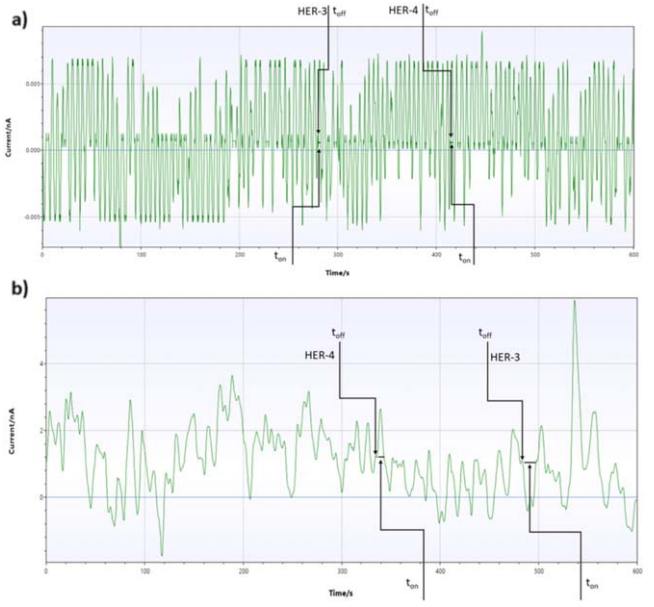

Figure 2. Examples of diagrams for the screening tests of tumoral tissue using the stochastic sensors based on: (a) AuNPs/α-CD-nGr and (b) spheroidal Cu/α-CD-nGr.

processes of HER3 and HER4, their sign changes and then they exit the channel. Calibration equations ($1/t_{on} = a + bxC_{HER3/HER4}$) were derived using the linear regression methods.

2.5. Biological samples

For the purpose of this investigation, four distinct kinds of biological samples were collected from patients who had previously been diagnosed with gastric cancer. These samples were then used. At the time that the patients' samples were being collected for this study, none of the patients who were enrolled in the study were undergoing any kind of treatment for gastric cancer. Tumoral tissue and whole blood samples were obtained from a local hospital, and in order to do so, an approval from the committee (numbers 32647/14.12.2018 and 3206/28.02.2019), was obtained, as well as informed consent from the enrolled patients. Before being used for stochastic sensing, the samples that were chosen were not treated in any way in advance of that process. Using the stochastic method outlined earlier, the unknown concentrations of HER3 and HER4 were determined using biological samples.

3. Results and discussion

3.1. Morphological and structural characterization

SEM microscopy was conducted to investigate the morphology of sensors' pastes, and the quantitative analysis/the elements quantification was carried out by EDX. The surface morphologies for the AuNPs/α-CD-nGr sensor is presented in figure 3 and those for the spheroidal Cu/α-CD-nGr sensor is presented in figure 4. The EDX spectra and related quantification are presented in figure 5.

In figure 3, the surface morphology of the paste is depicted as several layers of irregularly shaped flakes of varying sizes, whereas in figure 4, the surface morphology of the paste based on spheroidal Cu consists of randomly oriented sheets that stack to form a three-dimensional porous framework.

From the quantitative analysis, it can be seen that the predominant element is C for both materials studied, and in the case of the Cu/α-CD-nGr spheroidal sample, the presence of the Cu element is additionally noted (0.15 At%) (figure 5).

3.2. Performance characteristics of the nanoplatforms

Stochastic sensors rely on reversible molecular bindings to the walls of the pores/channels of modified matrices, which represent the underlying principle of their operation. After applying a constant 170 mv potential, the conductivity of the pore is measured, and the results are depicted using the diagrams provided.

The parameters of the nanoplatforms are shown in table 1. The signatures obtained for HER3 and HER4 are different for each of the nanoplatform used, proving that the nanoplatforms can be used for the simultaneous assay of HER3 and HER4. For the assay of HER3, in comparison to the AuNPs/α-CD-nGr sensor, the spheroidal Cu/α-CD-nGr sensor yielded a lower limit of determination (of fg ml^{-1} magnitude order) (the limit of determination was determined

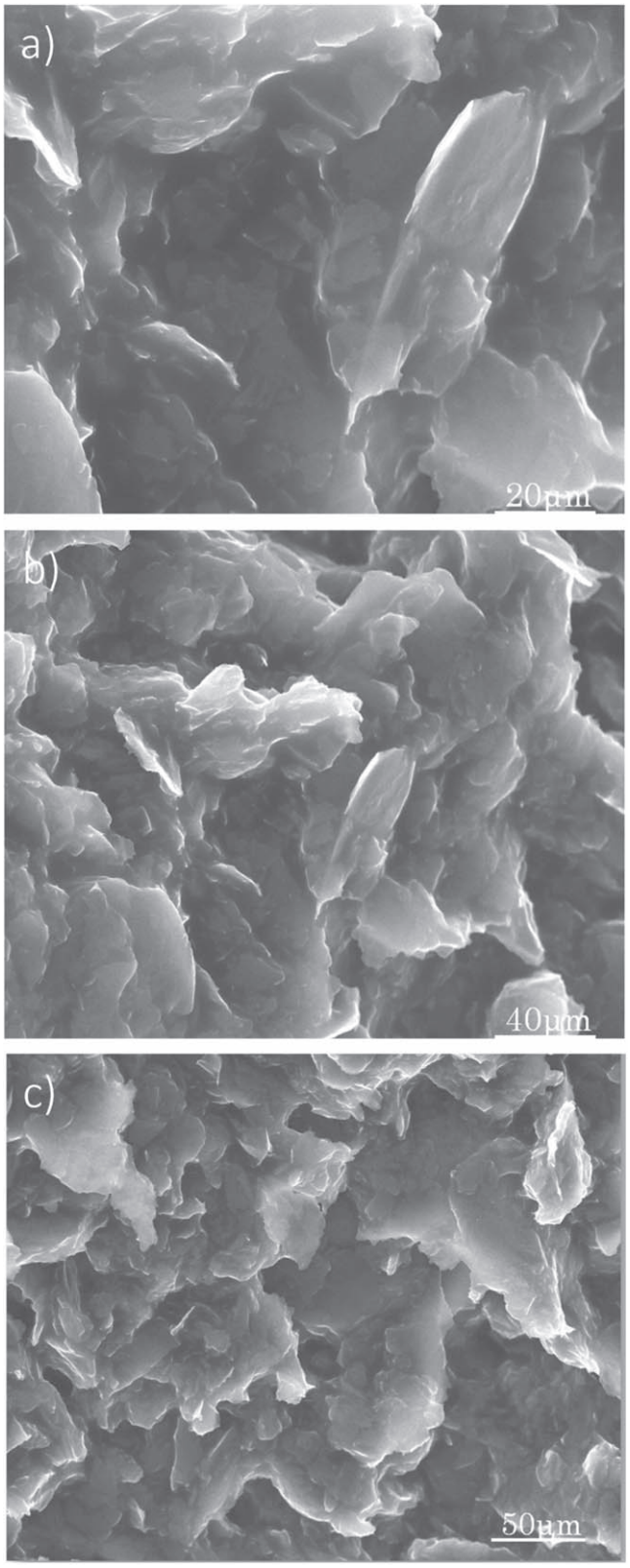

Figure 3. Representative SEM micrographs of AuNPs/α-CD-nGr at different scales (20 μm (a), 40 μm (b), 50 μm (c)).

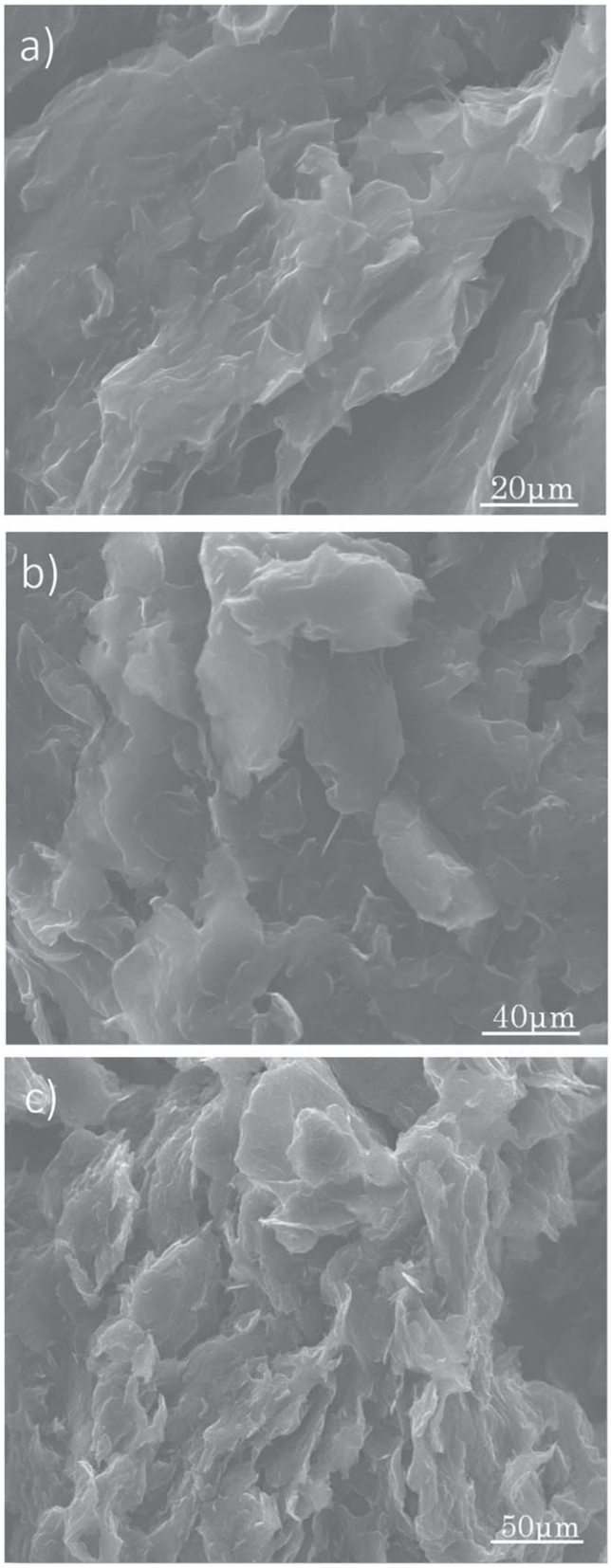

Figure 4. Representative SEM micrographs of spheroidal Cu/α-CD-nGr at different scales (20 μm (a), 40 μm (b), 50 μm (c)).

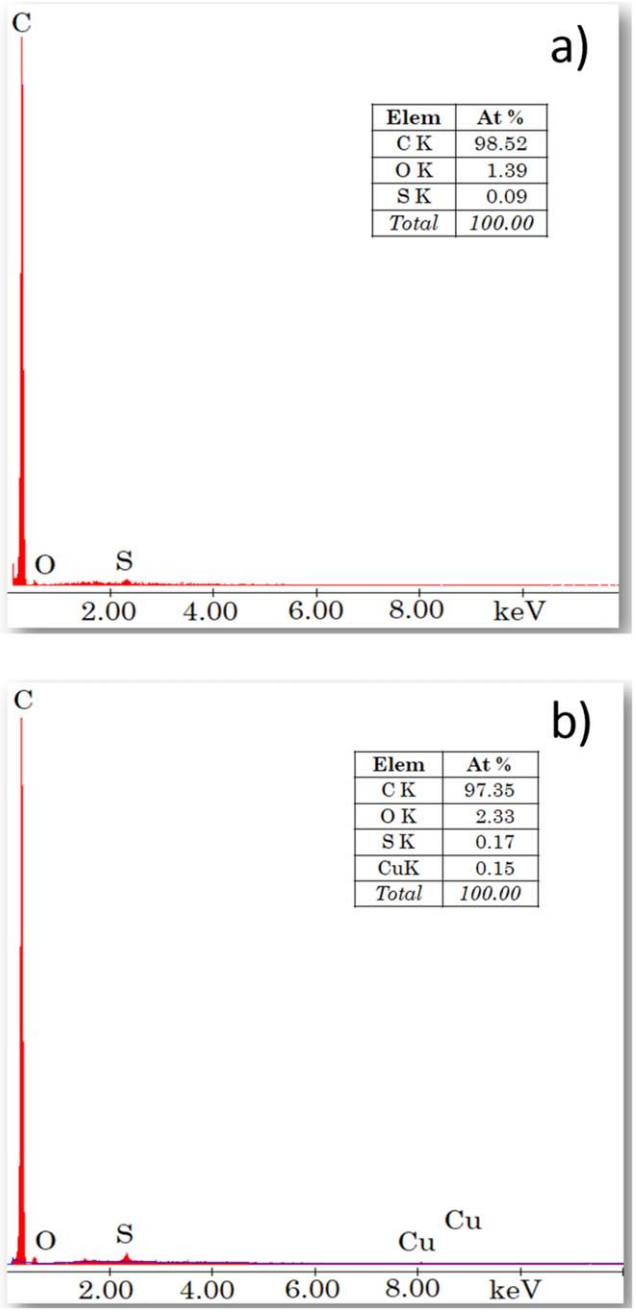

Figure 5. EDX spectra/element quantification of (a) AuNPs/α-CD-nGr and (b) spheroidal Cu/α-CD-nGr.

accordingly with the IUPAC guidelines [21] and it is the lowest value from the linear concentration range); also, the Cu/α-CD-nGr sensor exhibited a higher sensitivity and a wider linear concentration range. For the assay of HER4, the metal used in the sensor's design did not *influence* the limit of determination; the sensitivity had also the same magnitude order, but wider linear concentration range was obtained when the sensor based on Cu/α-CD-nGr was used. The linear concentration ranges were sufficiently broad to accommodate

Ta **I.** Performance characteristics of the nanoplatforms for the assay of HER3 and HER4 ($N = 10$).

Nanoplatforms using stochastic sensors based on	Working	ntration range l^{-1})	Calibration equation and r[a]	t_{off} (s)	Sensitivity ($s^{-1}/\mu g\ ml^{-1}$)	Limit of determination (g ml^{-1})
			HER3			
Spheroidal Cu/α-CD-nGr	1×1	-1×10^{-9}	$1/t_{on} = 0.24(\pm 0.02) + 3.89(\pm 0.03) \times 10^6$C $R = 0.9997$	1.2(± 0.1)	3.89×10^6	1×10^{-15}
AuNPs/α-CD-nGr	1×1	-1×10^{-8}	$1/t_{on} = 0.82(\pm 0.03) + 84.17(\pm 0.01)$C $R = 0.9999$	1.9(± 0.2)	84.17	1×10^{-10}
			HER4			
Spheroidal Cu/α-CD-nGr	1×10^{-15}–1×10^{-8}		$1/t_{on} = 0.22(\pm 0.02) + 6.17(\pm 0.02) \times 10^6$C $R = 0.9999$	2.3(± 0.2)	6.17×10^6	1×10^{-15}
AuNPs/α-CD-nGr	1×10^{-15}–1×10^{-9}		$1/t_{on} = 0.21(\pm 0.01) + 8.98(\pm 0.03) \times 10^6$C $R = 0.9999$	1.1(± 0.1)	8.98×10^6	1×10^{-15}

[a] $\langle 1/t_{on} \rangle = s^{-1}$; $\langle C \rangle$—concentration = $\mu g\ ml^{-1}$; $<r>$—correlation coefficient

Table 2. Performance characteristics of the nanoplatforms using stochastic sensors and other sensors used to date.

Sensor	Working concentration range (g ml^{-1})	LOQ (g ml^{-1})	References
	HER3		
Spheroidal Cu/α-CD-nGr	1.00×10^{-15}–1.00×10^{-9}	1.00×10^{-15}	This work
AuNPs/α-CD-nGr	1.00×10^{-10}–1.00×10^{-8}	1.00×10^{-10}	This work
MD/Gr-TiO_2-Au	1.00×10^{-15}–1.00×10^{-11}	1.00×10^{-15}	[22]
MD/Gr-TiO_2	1.00×10^{-14}–1.00×10^{-10}	1.00×10^{-14}	[22]
Immunological biosensor	2.00×10^{-13}–1.40×10^{-12}	2.00×10^{-13}	[23]
IN/AuNP-SWCNT	1.00×10^{-9}–1.00×10^{-6}	1.00×10^{-9}	[24]
IQ/AuNP-SWCNT	1.00×10^{-8}–1.00×10^{-6}	1.00×10^{-8}	[24]
HD/AuNP-SWCNT	1.00×10^{-9}–1.00×10^{-6}	1.00×10^{-9}	[24]
TEX/AuNP-SWCNT	1.00×10^{-9}–1.00×10^{-6}	1.00×10^{-9}	[24]
IN/AuNP-MWCNT	1.00×10^{-9}–1.00×10^{-2}	1.00×10^{-9}	[11]
IQ/AuNP-MWCNT	1.00×10^{-9}–1.00×10^{-7}	1.00×10^{-9}	[11]
HD/AuNP-MWCNT	1.00×10^{-9}–1.00×10^{-7}	1.00×10^{-9}	[11]
TEX/AuNP-MWCNT	1.00×10^{-7}–1.00×10^{-5}	1.00×10^{-7}	[11]
	HER4		
Spheroidal Cu/α-CD-nGr	1.00×10^{-15}–1.00×10^{-8}	1.00×10^{-15}	This work
AuNPs/α-CD-nGr	1.00×10^{-15}–1.00×10^{-9}	1.00×10^{-15}	This work
MD/Gr-TiO_2-Au	1.00×10^{-15}–1.00×10^{-6}	1.00×10^{-15}	[22]
MD/Gr-TiO_2	1.00×10^{-14}–1.00×10^{-10}	1.00×10^{-14}	[22]
IN/AuNP-SWCNT	1.00×10^{-9}–1.00×10^{-5}	1.00×10^{-9}	[24]
IQ/AuNP-SWCNT	1.00×10^{-8}–1.00×10^{-6}	1.00×10^{-8}	[24]
HD/AuNP-SWCNT	1.00×10^{-7}–1.00×10^{-5}	1.00×10^{-7}	[24]
TEX/AuNP-SWCNT	1.00×10^{-9}–1.00×10^{-5}	1.00×10^{-9}	[24]
IN/AuNP-MWCNT	1.00×10^{-9}–1.00	1.00×10^{-9}	[11]
IQ/AuNP-MWCNT	1.00×10^{-9}–1.00×10^{-1}	1.00×10^{-9}	[11]
HD/AuNP-MWCNT	1.00×10^{-8}–1.00×10^{-1}	1.00×10^{-8}	[11]
TEX/AuNP-MWCNT	1.00×10^{-9}–1.00×10^{-2}	1.00×10^{-9}	[11]
Affimer-based electrochemical biosensor	2.72×10^{-13}–2.885×10^{-8}	2.72×10^{-13}	[25]

both healthy individuals and individuals with varied stages of stomach cancer. Different biomarker levels show that they can be detected simultaneously in biological samples. Compared to other works [22], in this case, the sensitivity of the nanoplatforms using stochastic sensors is comparable and even better than the forementioned work and the standard method, ELISA (1.52×10^{-11} g ml^{-1} for HER3 and 1.25×10^{-10} g ml^{-1} for HER4). Compared to other stochastic sensors used to date for the assay of HER3 and HER4 [11, 22, 24], the nanoplatform using the sensor based on α-CD-nGr and modified with spheroidal Cu had lower limits of determination and covered larger linear concentration ranges.

Table 2 presents a comparison between the performance characteristics of the nanoplatforms using stochastic sensors and other sensors from the literature.

The calibration curves for the assay of HER3 and HER4 in biological samples are shown in figure 6.

3.3. Reproducibility and stability of the stochastic sensors

Each sensor was the subject of reproducibility studies. Consequently, 10 of each type of sensor were produced using the method described in the section on sensor design. When immersed in solutions of pH 7.40 for HER3 and HER4, the sensitivities of each sensor were determined and compared. Each sensor's stability was evaluated as follows: As described in the section on stochastic sensor design, 20 of each type of sensor was stored. The response of each of the sensors was evaluated, and the sensitivities were compared; a variation of 0.02% was recorded for each type of sensor, proving the reproducibility of the sensors' design. Each day, a new sensor was removed from storage and immersed in solutions containing HER3 and HER4 of varying concentrations at pH 7.40; the sensitivity of each measurement was recorded for comparison after one month, when the entire batch of sensors has been employed. End-of-period results indicated a high degree of stability of the electrodes over time, as the change in sensitivity over time was 0.07% versus the initial sensitivity for spheroidal Cu/α-CD-nGr and 0.05% versus the initial sensitivity for AuNPs/α-CD-nGr.

3.4. Selectivity

The measured t_{off} values for a variety of possible interferences indicate the selectivity of the two proposed stochastic sensors. Examined as potential interferents were HRG-α, HER1, HER2, p53, and CEA. Given that the signatures of the selected chemicals differ from those of the relevant

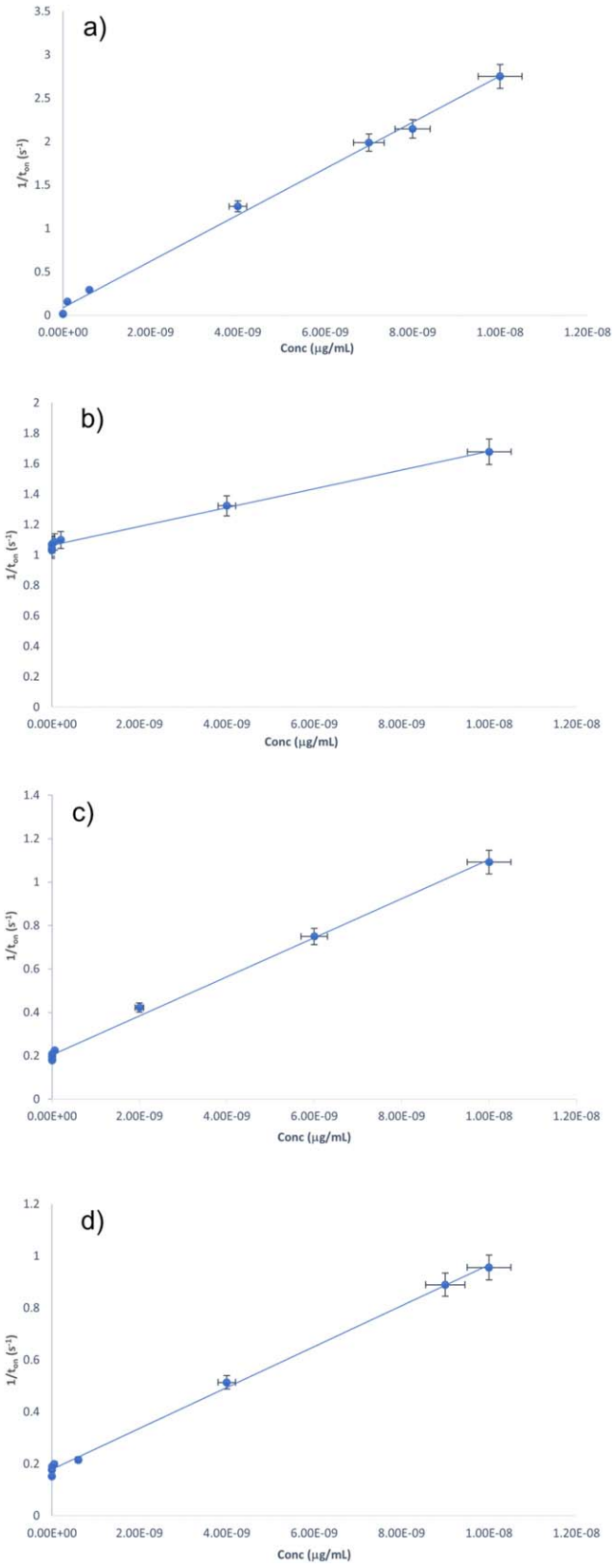

Figure 6. Calibration curves of the stochastic sensor based on spheroidal Cu/α-CD-nGr for the assay of (a) HER3, and (b) HER4 in whole blood samples, and for the stochastic sensor based on AuNPs/α-CD-nGr for the assay of (c) HER3, and (d) HER4 in whole blood samples.

biomarkers, table 3 demonstrates that none of them hinders the detection of HER3 and HER4.

3.5. HER3 and HER4: molecular identification and quantification

Two stochastic sensors were utilized for the rapid screening of biological samples, including tumoral tissue and whole blood, from patients with gastric cancer. HER3 and HER4 were identified in the diagrams (figures 1 and 2) based on their signatures before the matching t_{on} was read and utilized in the stochastic mode to determine the concentration of HER3 and HER4. The assay results for the biological samples (five whole blood and five tumoral tissue samples) are presented in figures 7 and 8. One can find very good correlations between the outcomes.

A paired Student's *t* test was performed with a level of confidence of 99.90%. The calculated *t* values for each sample type were less than the tabulated value, indicating that there is no statistically significant difference between the results obtained using the proposed nanoplatforms because the calculated values were 1.98 for HER3 and 1.93 for HER4 in whole blood and 1.91 for HER3 and 2.01 for HER4 in tumoral tissue kand that these can be relied upon for the molecular identification and quantification of HER3 and HER4 in the chosen biological samples. In addition, the validation was conducted using the conventional addition method, which involved the addition of known quantities of HER3 and HER4 to each type of biological sample, including whole blood and tumoral tissue. Extremely high recovery values were obtained when HER3 and HER4 were identified in two distinct types of biological material. These results demonstrated that the proposed nanoplatforms can be used to identify and quantify HER3 and HER4 in biological samples with reliability. The recovery tests indicate that the proposed nanoplatforms can be used with confidence for the assay of HER3 and HER4 in whole blood and tumoral tissue, as all recoveries were greater than 98.00% and the RSD values were less than 1.00%.

4. Conclusions

Two nanoplatforms were suggested for the fast detection of two biomarkers, HER3 and HER4 in two types of biological samples (whole blood and tumoral tissue). The best results were obtained when the nanoplatform based on spheroidal Cu/α-CD-nGr was used, for which the recovery was greater than 98.00% and the RSD value was less than 1.00%. When used for screening tests on whole blood and tumor tissue, the sensors, incorporated in nanoplatforms, are effective and cost-efficient instruments. The primary advantage of these nanoplatforms consists of smartphone detection, which simultaneously detects the two biomarkers of interest, thus, enabling the analysis of a panel of biomarkers in biological samples. Utilizing a screening test for the rapid detection of gastric cancer and the ability to detect it at an early stage is their distinguishing feature. In the not-too-distant future, these nanoplatforms offer a variety of possible

Table 3. Selectivity of the nanoplatforms using stochastic sensors used for the determination of HER3 and HER4.

Nanoplatforms using stochastic sensors based on α-CD and nGr and modified with	HER3	HER4	HRG- α	HER1	HER2	p53	CEA
	Signature (t_{off}) (s)						
AuNPs	1.9	1.1	0.8	1.6	4.2	3.3	1.7
Spheroidal Cu	1.2	2.3	1.0	1.4	1.3	4.2	1.9

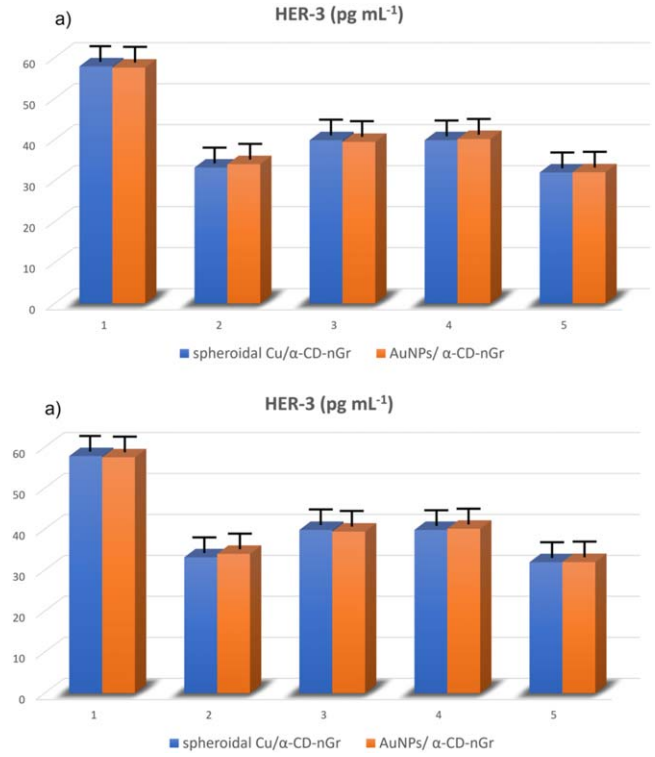

Figure 7. The results of the screening tests of HER3 (a) and HER4 (b) in whole blood samples ($N = 10$).

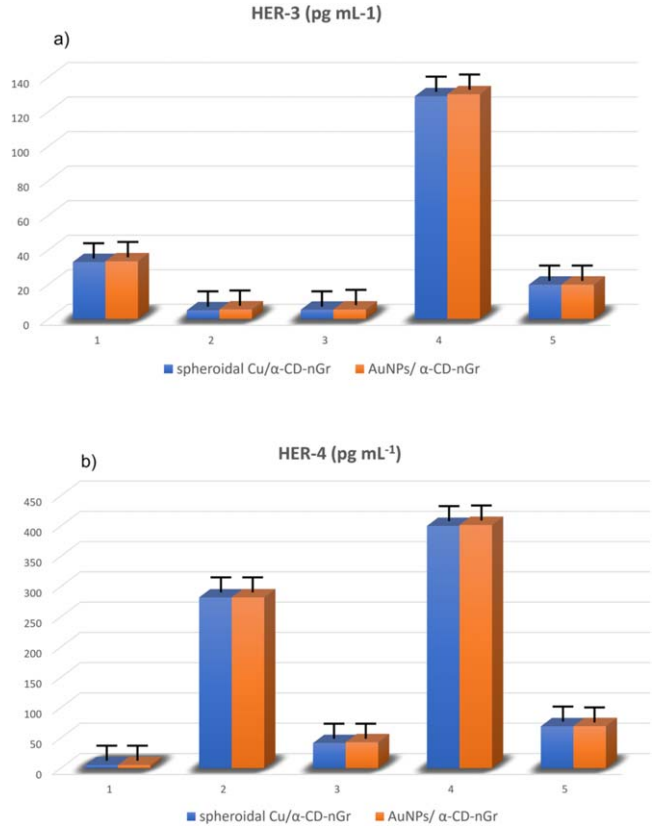

Figure 8. The results of the screening tests of HER3 (a) and HER4 (b) in tumoral tissue samples ($N = 10$).

uses because they are compatible with smartphone devices. These applications include their implementation in operating rooms, routine analysis of HER3 and HER4, and gastric cancer patients' treatment regimens.

Acknowledgments

This work was supported by a grant of the Ministry of Research, Innovation and Digitization, CNCS/CCCDI—UEFISCDI, project number PN-III-P2-2.1-PED-2021-0390, within PNCDI III.

Data availability statement

The data cannot be made publicly available upon publication because the cost of preparing, depositing and hosting the data would be prohibitive within the terms of this research project. The data that support the findings of this study are available upon reasonable request from the authors.

Ethics committee

The samples were obtained from the Emergency Clinical Hospital of County Targu-Mures, which was granted permission to conduct the research by the Ethics Committee with the number 32647/14.12.2018, and from the Clinical Hospital County Targu-Mures, which was granted permission to conduct the research by the Ethics Committee with the number 3206/28.02.2019. Informed consent was obtained from all patients.

ORCID iDs

Damaris-Cristina Gheorghe https://orcid.org/0000-0002-6430-2177
Raluca-Ioana Stefan-Van Staden https://orcid.org/0000-0001-8244-2483

Ruxandra-Maria Ilie-Mihai https://orcid.org/0000-0002-2285-9583
Paula Sfirloaga https://orcid.org/0000-0002-8947-3810

References

[1] Ocana A and Pandiella A 2013 *Curr. Pharm. Des.* **19** 808
[2] Du Z and Lovly C M 2018 *Mol. Cancer* **17** 58
[3] Arteaga C L and Engelman J A 2014 *Cancer Cell* **25** 282
[4] Hynes N E and Lane H A 2005 *Nat. Rev. Cancer* **5** 341
[5] Li Q, Zhang R, Yan H, Zhao P, Wu L, Wang H, Li T and Cao B 2017 *Oncotarget* **8** 67140
[6] Vivanco I and Sawyers C L 2002 *Nat. Rev. Cancer* **2** 489
[7] Wu X, Chen Y, Li G, Xia L, Gu R, Wen X, Ming X and Chen H 2014 *Med. Oncol.* **31** 903
[8] He X X, Ding L, Lin Y, Shu M, Wen J M and Xue L 2015 *J. Clin. Pathol.* **68** 374
[9] Abrahao-Machado L F and Scapulatempo-Neto C 2016 *World J. Gastroenterol.* **22** 4619
[10] Tang D, Liu C Y, Shen D, Fan S, Su X, Ye P, Gavine P R and Yin X 2014 *Onco Targets Ther.* **8** 7
[11] Cioates Negut C, Stefan-Van Staden R I and Sfirloaga P 2022 *Chemistry* **4** 1382
[12] Stefan-Van Staden R I, Comnea-Stancu I R, Surdu-Bob C C and Badulescu M 2015 *Nanoscale* **7** 15689
[13] Stefan-Van Staden R I, Musat O R, Gheorghe D C, Ilie-Mihai R M, Cioates Negut C and Sfirloaga P 2022 *Talanta Open* **6** 100151
[14] Ali M M, Aguirre S D, Xu Y, Filipe C D, Pelton R and Li Y 2009 *Chem. Commun. Camb. Eng.* **2009** 6640
[15] Parolo C and Merkoçi A 2013 *Chem. Soc. Rev.* **42** 450
[16] Le V T, Vasseghian Y, Dragoi E N, Moradi M and Mousavi Khaneghah A 2021 *Food Chem. Toxicol.* **148** 111931
[17] Yu X, Chen Y, Chang L, Zhou L, Tang F and Wu X 2013 *Sensors Actuators* B **186** 648
[18] Zhao Y, Zheng X, Wang Q, Zhe T, Bai Y, Bu T, Zhang M and Wang L 2020 *Food Chem.* **333** 127495
[19] Upadhyay S S, Gadhari N S and Srivastava A K 2020 *Biosens. Bioelectron.* **165** 112397
[20] Liu Z M, Yang Y, Wang H, Liu Y L, Shen G L and Yu R Q 2005 *Sensors Actuators* **106** 394
[21] Stefan-Van Staden R I, Gheorghe D C and Stoica R A 2022 *Sens. Diagn.* **1** 977
[22] Stefan-Van Staden R I and Gheorghe D C 2022 *Micromachines* **13** 1749
[23] Canbaz M Ç, Şimşek Ç S and Sezgintürk M K 2014 *Anal. Chim. Acta* **814** 31
[24] Stefan-Van Staden R I, Negut C C and Sfirloaga P 2023 *J. Electrochem. Soc.* **170** 037503
[25] Zhurauski P, Arya S K, Jolly P, Tiede C, Tomlinson D C, Ferrigno P K and Estrela P 2018 *Biosens. Bioelectron.* **108** 8